Vision Research 50 (2010) 1882–1890

Contents lists available at ScienceDirect

Vision Research

journal homepage: www.elsevier.com/locate/visres

Global saccadic adaptation

Martin Rolfs [a,b,*], Tomas Knapen [b,c], Patrick Cavanagh [b]

[a] New York University, Department of Psychology, 6 Washington Place, 10003 New York, NY, USA
[b] Université Paris Descartes, Laboratoire Psychologie de la Perception, 45 rue des Saints-Pères, 75006 Paris, France
[c] University of Amsterdam, Department of Psychology, Roeterstraat 15, 1018 WB Amsterdam, The Netherlands

ARTICLE INFO

Article history:
Received 20 December 2009
Received in revised form 10 June 2010

Keywords:
Motor plasticity
Motor learning
Adaptation
Eye movements
Saccade
Oculomotor control

ABSTRACT

Our actions need constant calibration to arrive accurately at locations of their intended goals; errors in execution must drive rapid adjustments. As an example, saccadic eye movements are vital for bringing objects of interest into the high-acuity center of vision and they must be continually tuned to compensate for ongoing changes in body, muscle strength and neural variability. This adaptation of eye movement responses can be induced artificially by systematically displacing the saccade targets by a constant proportion during each saccade. Observers do not notice these shifts and yet the oculomotor system does, rapidly compensating for the landing error until the saccades finally land close to the artificially displaced target. This recalibration has been described as spatially selective, dropping off with distance in direction and amplitude from the adapted saccade vector. However, we now report that this local adaptation property is a consequence of adapting to only one direction at a time, the method generally used in previous studies. When we induced adaptation in all directions, using a quasi-random walk where each target was displaced 25% back toward to the previous fixation, we found strong, spatially generalized adaptation that could not be accounted for by an accumulation of many vector-specific adaptations. This global adaptation is a plausible strategy for calibration given the absence of any obvious growth changes or muscle deficits that would lead to vector specific losses and it provides a robust model for testing motor calibration.

1. Introduction

Plasticity is a fundamental prerequisite of goal-directed behavior as it maintains an accurate calibration of motor acts to perceptual input. The necessity of this calibration process is particularly evident for saccades, the rapid eye movements that we generate several times per second to bring objects of interest onto the fovea, the site of high visual acuity. It has been shown that if the position of a saccade target is systematically shifted during several successive saccades, its amplitude adapts to compensate for the shift (McLaughlin, 1967). This recalibration process is known as saccadic adaptation (Hopp & Fuchs, 2004) and takes place while the observer is often oblivious to the intra-saccadic displacements (Bridgeman, Hendry, & Stark, 1975). Saccadic adaptation is considered to be quite local—specific to the adapted vector and dropping off quickly with distance in polar coordinates. This vector-specificity is a robust finding, shown consistently in monkeys (Deubel, 1987; Noto, Watanabe, & Fuchs, 1999; Straube, Fuchs, Usher, & Robinson, 1997; Watanabe, Noto, & Fuchs, 2000) and humans (Albano, 1996; Alahyane, Devauchelle, Salemme, & Pélisson, 2008; Collins, Doré-Mazars, & Lappe, 2007; Deubel, 1987; Frens & van Opstal, 1994; Miller, Anstis, & Templeton, 1981). In fact, opposite gain changes can be obtained for saccades in the same direction if their amplitudes differ sufficiently (Watanabe et al., 2000). Based on these results it has been claimed that a critical neural substrate determining saccadic adaptation lies in those oculomotor structures where saccades are still represented as vectors, e.g., the superior colliculus (SC) or the frontal eye fields (Hopp & Fuchs, 2004, 2006), rather than in more peripheral structures that implement their global horizontal and vertical component signals sent to the extraocular muscles (Sparks, 2002). Indeed, recent evidence suggests a causal role of the SC in sending instructive signals for saccadic adaptation (Kaku, Yoshida, & Iwamoto, 2009).

While the specificity of these processes is impressive, the function of vector-specific saccadic adaptability has been puzzling. Saccade performance is affected by many factors such as fluctuations in alertness due to fatigue (Barton, Jama, & Sharpe, 1995), rest, the consumption of stimulating substances, as well as long-term factors like growth, aging (Warabi, Kase, & Kato, 1984), strengthening, weakening or even palsy of (Abel, Schmidt, Dell'osso, & Daroff, 1978; Kommerell, Oliver, & Theopold, 1976) or lesions to the extra-

* Corresponding author at: Université Paris Descartes, Laboratoire Psychologie de la Perception, 45 rue des Saints-Pères, 75006 Paris, France. Fax: +33 1 42863322.
E-mail address: martin.rolfs@gmail.com (M. Rolfs).
URL: http://www.martinrolfs.de (M. Rolfs).

0042-6989/$ - see front matter © 2010 Elsevier Ltd. All rights reserved.
doi:10.1016/j.visres.2010.06.010

ocular muscles (Optican & Robinson, 1980; Snow, Hore, & Vilis, 1985). All of these factors have global effects on saccades, but the accumulation of adaptation of saccades in all different directions independently would be slow and inefficient (Scudder, Batourina, & Tunder, 1998). Moreover, due to the statistical nature of the external and internal environments, the errors that saccadic adaptation corrects occur at many different scales in both time and space. Because of this generality, it is not surprising that motor adaptation occurs at many different timescales (Körding, Tenenbaum, & Shadmehr, 2007; Srimal, Diedrichsen, Ryklin, & Curtis, 2008), and spatially general adaptation, the opposite of directionally specific adaptation, may also be expected. In fact, a recent study by Garaas, Nieuwenhuis, and Pomplun (2008) reported rapid changes in saccade gain when a visual search display was gaze-contingently shifted in the direction opposite each eye movement. Pursuing other goals, this study did not investigate whether generalized recalibration relies on mechanisms of plasticity that are different from those studied in the saccadic adaptation literature.

Introducing a new, generalized version of the classical adaptation paradigm (McLaughlin, 1967), we now provide detailed evidence for a separate, global recalibration process of saccade gains that accumulates more strongly than vector-specific adaptation. Twelve human observers continuously re-fixated a visual target stepping in a quasi-random walk across the display (Fig. 1A, top row), allowing us to measure the baseline gain of saccades for different directions and amplitudes before adaptation (distribution of possible target steps shown in Fig. 1B). One hundred of these test trials were followed by a block of 200 adaptation trials (Fig. 1A, middle row), which differed across the three different conditions. The distribution of possible target steps in adaptation trials are shown in Fig. 1C. During *Global adaptation* (Fig. 1A and C, left columns), the saccade target continued stepping along a quasi-random path. However, the presaccadic target was displaced during each saccade to end up 25% closer to the initial fixation position (back-step), where it was seen by the observer after the saccade. During *One-way adaptation* (Fig. 1A and C, middle columns), only 8° saccades in one direction were adapted, while return saccades in the opposite direction did not trigger a trans-saccadic back-step of the target. In this condition we replicated the classical finding that adaptation drops off as a function of saccade direction. Finally, during *Two-way adaptation* (Fig. 1A and C, right columns), a condition designed to control if consistent visual feedback across all target steps explains the data obtained in the Global adaptation paradigm, we adapted 8° saccades in two opposite directions at the same time. Following the adaptation block, we tested for changes in saccade amplitudes by running another block of 100 test trials, which where randomly interleaved with another 200 adaptation trials to keep up adaptation (Fig. 1A, bottom row). Comparing the time course and spatial transfer of adaptation across these conditions, we reveal a general recalibration of saccade gains, pointing to basic saccadic adaptation mechanisms at the final stages of oculomotor processing whose neurophysiological correlates have yet to be explored.

2. Methods

2.1. Observers

We tested 12 observers (6 female, age 19–32, 8 right-eye dominant, 10 right-handed); all but author TK and colleague RA were naïve to the goals of the study. They had normal or corrected-to-normal vision and gave their informed consent before study participation. The experiments were conducted in accordance with the Declaration of Helsinki.

2.2. Experimental setup and stimuli

Observers sat in a silent and dimly lit room with the head positioned on a chin rest, 63 cm in front of a computer screen. Stimuli were red (3.5 cd/m^2) and black (0.15 cd/m^2) 0.2°-diameter dots on a gray background (16.5 cd/m^2), presented on a 22" Formac ProN-

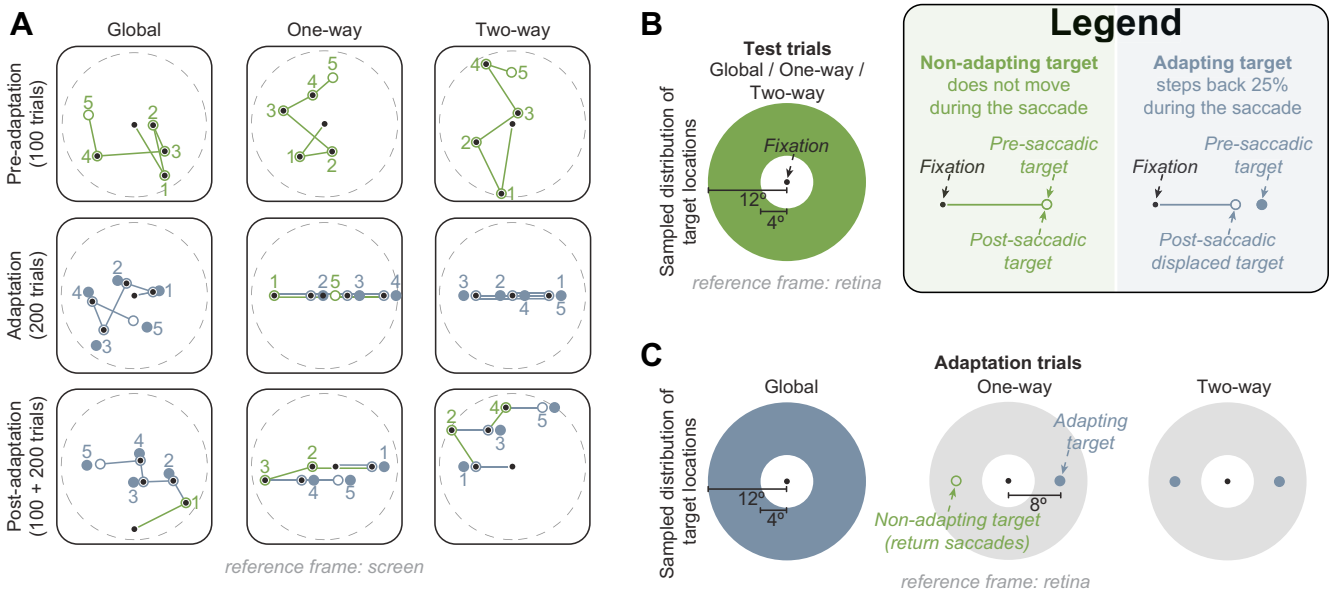

Fig. 1. Experimental procedure in the three adaptation conditions. **A** For each of the three blocks of trials in an experiment, five subsequent example target steps (see Legend) are shown as they occurred on the screen. Numbers are placed next to the pre-saccadic target. In the One-way and Two-way adaptation blocks, target vectors fall on the same path, because only horizontal saccades were used. **B** and **C** Illustration of the pool of target steps sampled in test and adaptation trials, respectively, for each of the three adaptation conditions. Filled green and blue regions indicate that target steps distributed across the depicted annulus, including any direction between 0 and 359° and any amplitude between 4 and 12°. For comparison, filled gray regions highlight these annuli in the depiction of One-way and Two-way adaptation trials. **L**egend Two types of target steps used; Non-adapting (green): single saccade-triggering target step; Adapting (blue): saccade-triggering target step, stepped back 25% intra-saccadically. (For interpretation of the references to color in this figure legend, the reader is referred to the web version of this article.)

itron 22800 screen with a spatial resolution of 768 × 1024 pixels run at a vertical refresh rate of 145 Hz. Gaze position of the dominant eye was recorded and available online using an EyeLink 1000 Desktop Mount (SR Research, Osgoode, Ontario, Canada) with an average spatial resolution of 15 to 30 min-arc, sampling at 1000 Hz. The experiment was controlled by an Apple MacPro computer; manual responses were recorded through a standard keyboard. The software controlling stimulus presentation and response collection was implemented in MATLAB (MathWorks, Natick, Massachusetts, USA), using the Psychophysics (Brainard, 1997; Pelli, 1997) and EyeLink toolboxes (Cornelissen, Peters, & Palmer, 2002).

2.3. Procedure

Observers performed three conditions, each separated by at least a week, their order counterbalanced across observers. An experiment consisted of three blocks of trials, a pre-adaptation block (100 test trials), an adaptation block (200 adaptation trials), and a post-adaptation block (100 test trials and 200 adaptation trials randomly interleaved, to maintain adaptation at a constant level). Fig. 1A shows examples of the paths these target steps created. On every trial, the direction of the saccade to be made was drawn randomly from the pool of possible target steps, illustrated in Fig. 1B and C, with the constraint that the fixation target was displaced within the invisible borders of a circular field (diameter of 24° centered on the screen; dashed line in Fig. 1A). The first trial started from the screen center and subsequent trials continued from the latest target position. In test trials, target steps could be in any direction (0–359°, in steps of 1°), with an amplitude range of 4–12° (in steps of 0.04°, the size of a pixel on the screen). In adaptation trials, possible target steps differed between experiments. In the Global adaptation experiment, we sampled from the same range of target steps in adaptation trials as in test trials, thus all adaptation trials included an intra-saccadic back-step. In the One-way adaptation experiment, the 200 adaptation trials consisted of 8° target steps, either to the left (six observers) or to the right (remaining six observers), that were followed by an intra-saccadic back-step and an equivalent amount of return target-steps in the opposite direction. These non-adapting trials were interspersed for two reasons: to remain within the circular area and to replicate traditional studies on saccadic adaptation, in which adapting target steps are usually followed by a (non-adapted) return saccade to a fixation location. Finally, the Two-way adaptation experiment was identical to the One-way, except that we adapted 8° saccades to the left and to the right at the same time. Hence, all saccade-triggering target-steps were followed by a back-step of the target during the saccade.

Each trial started with a small red fixation target. When fixation had been detected continuously for 200 ms in a circular fixation area (diameter of 3° centered on the target), the target turned black and, after a fixation period of 500–1000 ms, jumped to a new position. Observers were instructed to follow the target with the eyes. In test trials, target position was not changed during the saccade. Eye position was monitored throughout the trial. In adaptation trials sampling an adapting saccade target vector, saccades triggered an immediate back-step of the target stimulus, placing it 25% closer to its previous location. Saccades were detected online as soon after target presentation as the eyes left the boundary of the fixation area. The next trial started 750 ms later. When fixation broke due to blinks or large eye movements during the fixation period, a warning appeared on the screen asking observers to maintain fixation and the trial was rerun immediately.

In every back-step trial the target was displaced before the eye landed, during saccadic suppression of displacement (Bridgeman et al., 1975). Observers were instructed to press a key immediately whenever they saw a displacement of the target during the eye movement. This occurred in 1.8%, 1.6%, and 0.9% of all back-step trials (hits), primarily during the first trials in the adaptation block, and in 0.5%, 0.7%, and 1.0% of the non-adapting trials (false alarms) in One-way, Two-way, and Global adaptation conditions, respectively. Fig. 2 shows the frequency of perceptual reports across the entire experiments.

The first two blocks were preceded by a standard nine-point grid calibration–validation procedure of the eye tracker. During the second and third block, i.e., after adaptation had started, calibration was repeated whenever fixation could no longer be detected in the fixation area (due to blinks or anticipatory eye movements). To prevent the incorporation of saccadic adaptation in the calibration, eye positions on calibration targets were accepted manually and only after several seconds.

2.4. Data analysis

All data of observers where One-way adaptation was applied to leftward saccades was mirrored along the vertical axis and then underwent a common analyses scheme with the data of observers where the adaptation was applied to rightward saccades. Offline saccade detection was based on an algorithm described by Engbert and Mergenthaler (2006). Smoothed velocities were computed using a moving average over five subsequent eye position samples in a trial. Saccades were detected as outliers in 2D-velocity space, exceeding the median velocity by 5 SD for at least 8 ms (eight subsequent samples). Overshoots in saccades often result in the detection of two saccades, thus events separated by 20 ms or less were merged into a single saccade. Response saccades were defined as the first saccade that brought the eye to a circular region around the presaccadic target with a radius of half its eccentricity. We excluded 4.6% of all trials from further analyses because blinks, no response saccade, or saccades larger than 1° before the response saccade were detected.

All confidence intervals were computed using standard bootstrapping techniques. For a given dependent variable, we generated 1000 bootstrap samples (sampling with replacement) from our original sample of 12 data sets. The variable's standard deviation across these 1000 bootstrap samples is a reliable estimator of the standard error of the population (Efron & Tibshirani, 1993); by multiplying it by 1.96, we obtained a 95% confidence interval. Hence, we can be 95% certain that it contains the true mean of the population. Where confidence intervals are reported for data curves (e.g., in Fig. 4), we first computed curves for each individual and then submitted these to the bootstrapping procedure.

The computation of baseline saccade gains (see Appendix A) as well as all smoothing was done using the nonparametric LOWESS procedure (Cleveland, 1979), a robust locally weighted regression

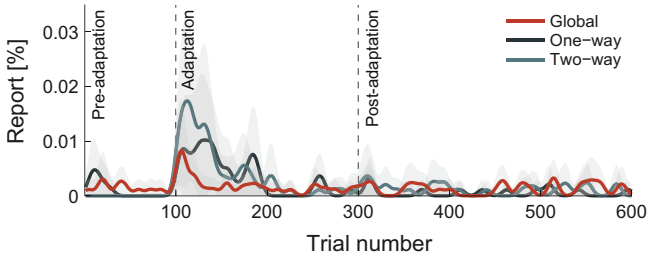

Fig. 2. The percentage of trials on which observers reported perceiving displacements of the target across the saccade is plotted as a function of trial number in the three subsequent blocks. Note that the area under each curve corresponds to the total percentage of trials with reports (temporal resolution is 1 trial), resulting in very low values at the *y*-axis. Shaded regions show 95% confidence intervals.

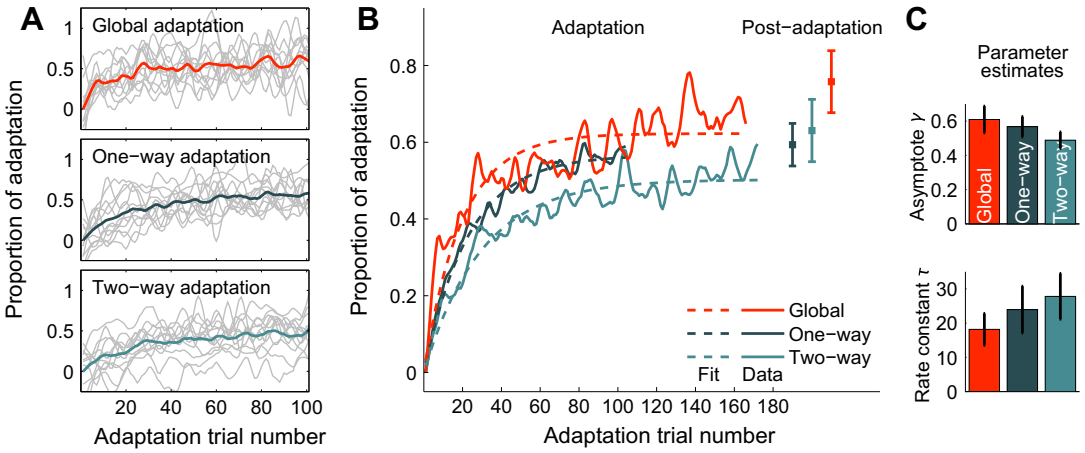

Fig. 3. Time course of adaptation. (**A**) The evolution of adaptation across adaptation trials in the adaptation block is plotted for each of the three conditions tested. Bold lines show the average across individual data (thin gray lines). (**B**) Superimposed average time courses of adaptation in the three conditions (solid lines) and exponential fits of these average curves (dashed lines). Note that although the Global condition includes saccades in all directions, the rate of adaptation was similar to that in the other conditions. The error bars to the right show the average proportion of adaptation in adaptation trials of the post-adaptation block with 95% confidence intervals. (**C**) Estimates of the rate constants and asymptotic proportions of adaptation for the three conditions tested. Error bars are standard errors of the mean.

with a bisquare weight function. The smoothness factor *f* was generally set to 0.3 (proportion of data used in fitting each value), except in the time course analyses where data were smoothed to a lesser extent to not average out fast changes in the proportion of adaptation. Here *f* was adjusted for each condition separately such that only the eight nearest data points contributed to each computed value.

3. Results

3.1. Baseline data

In the pre-adaptation test trials, our observers exhibited clear individual baseline patterns of saccadic under- or overshoots as a function of target direction. These patterns did not show systematic differences across conditions. However, because they varied considerably across observers and sessions, the proportion of adaptation was expressed relative to these baseline values. To this end, all saccade amplitudes were transformed to saccade gains (saccade amplitude divided by the target step amplitude), expressed as a proportion of potential adaptation (henceforth, proportion of adaptation), and baseline-corrected using the data collected in the pre-adaptation block (see Appendix A for a detailed description of this procedure). Full or 100% adaptation would bring the adapted saccades 75% of the distance to the target as the target was always stepped back by 25% before the saccade landed. Thus, proportions of 0 signify that saccades land close to the presaccadic target (where they would land before adaptation); proportions of 1 signify that saccades move the eyes only 75% of that amplitude, so that they land close to where the post-saccadic, displaced target is presented in adapting trials.

3.2. Time course of adaptation

First, we analyzed the evolution of adaptation across adaptation trials in the adaptation blocks of our experiments. Individual evolutions of the proportion of adaptation were smoothed and subsequently averaged across observers. Fig. 3A shows the resulting curves for each of the three conditions tested; individual data are plotted as thin gray lines in the background. For all three conditions, the proportion of adaptation changed rapidly over the first trials and decelerated continuously before reaching an asymptotic level of about 0.5–0.7 (corresponding to a 12.5–17.5% change in saccade gain). For comparison, we superimposed these curves in Fig. 3B. Evidently, the average change in adaptation in the Global condition was at least as fast as adaptation in the One-way condition even though many different directions were recalibrated rather than one principal direction.[1]

To compare the speed of adaptation across conditions in a quantitative manner, we drew 1000 bootstrap samples from the data pool, computed their averages, and for each of them fitted an exponential function of the form

$$\hat{\gamma}(t) = \gamma - \gamma e^{-\frac{t}{\tau}}, \tag{1}$$

where γ is the asymptotic proportion, τ is the rate constant of the adaptation process, and t denotes the trial. This function assumes that the average proportion of adaptation is zero in the first trial, which was set to be the case for each sample. The fits of this function to the original sample averages are shown as dashed lines in Fig. 3B; the average parameters (±95% confidence intervals) obtained are shown in Fig. 3C. While Global adaptation reached the highest asymptote, it also had the shortest rate constant, that is, it evolved at the highest speed. The asymptotic proportion of adaptation was slightly lower for One-way adaptation and again slightly lower for Two-way adaptation. Conversely, the rate constants obtained in these conditions were slightly longer than in the Global adaptation condition. These results suggest that despite the fact that only one or two saccade vectors were adapted at the same time, adaptation in these conditions was not faster than in the Global adaptation condition. It is also noteworthy that while the exponential fits describe well the evolution of adaptation in the One-way and Two-way conditions, they tend to underestimate both the initial speed and the asymptote of adaptation in the Global condition. The time course of Global adaptation was better fit by a power law function. Conducting similar analyses as the ones reported here using power law fits yielded the same pattern of results.

[1] We ensured the validity of this comparison by juxtaposing the time course of Global adaptation trials with target steps in the amplitude range of One-way adaptation (6.5–9.5°) to that of other amplitudes. Speed and magnitude of adaptation were virtually identical between these two subsets of trials, reassuring us that there was no systematic disadvantage for saccades in the medium amplitude range, hence, for the One-way condition.

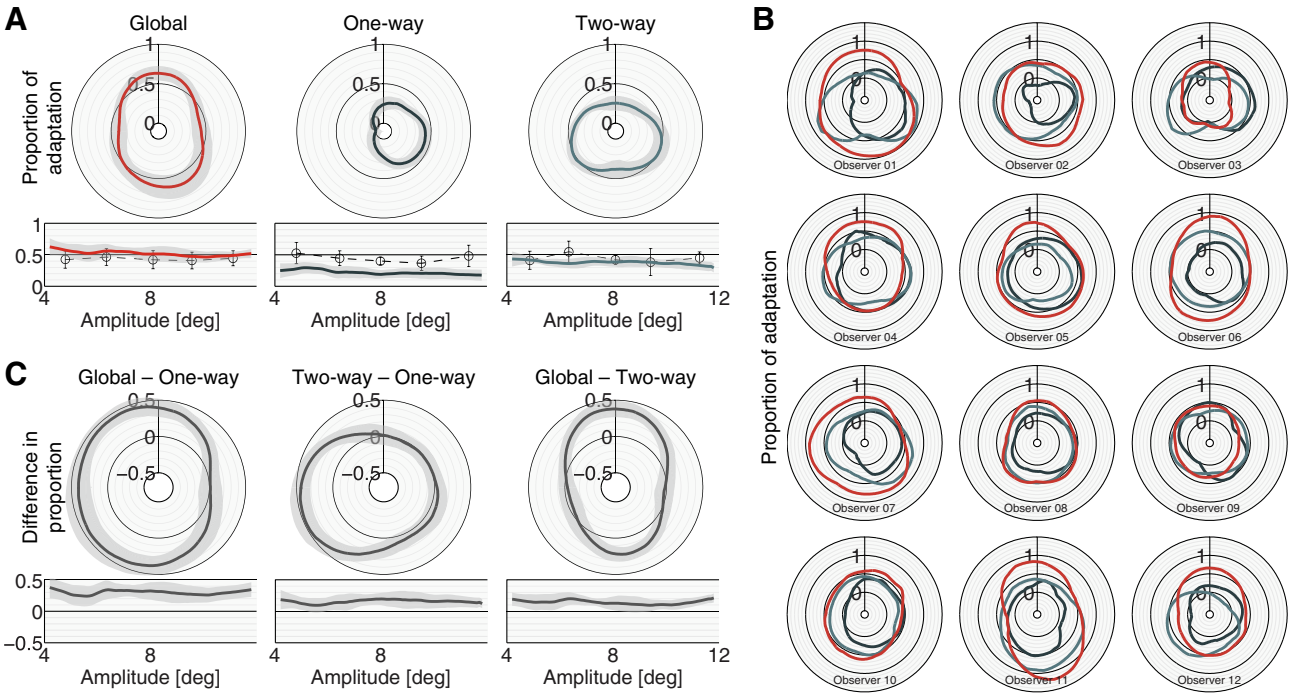

Fig. 4. Spatial extent of adaptation. **A** The proportion of adaptation after Global, One-way-, and Two-way adaptation is plotted as a function of target direction (upper panels) and amplitude (lower panels). Thick, colored lines represent the average across observers; shaded areas provide 95% confidence intervals. For comparison, dashed lines in the lower panels show the results for target directions within ±30° of the direction that was adapted in the One-way condition. Error bars are 95% confidence intervals. **B** Individual data as a function of target direction for the 12 observers contributing to the averages in A. **C** Differences in the proportion of adaptation between Global – One-way adaptation, Two-way – One-way adaptation, and Global – Two-way adaptation are shown as a function of target step direction (upper panels) and amplitude (lower panels). For each comparison, positive values signify stronger adaptation in the first compared to the latter condition. Shaded 95% confidence bands reveal significant inter-condition differences when they do not overlap with zero. (For interpretation of the references to color in this figure legend, the reader is referred to the web version of this article.)

3.3. Spatial extent of adaptation

The polar plots in Fig. 4A show the proportion of adaptation observed in the post-adaptation test trials as a function of target direction and averaged across 12 observers (means are shown with 95% confidence bands). In the Global adaptation condition (panel one in Fig. 4A) saccades of all directions were strongly adapted. The average proportion of adaptation obtained in this condition was about 0.5 (corresponding to a 12.5% change in saccade gain). In contrast, One-way adaptation resulted in a vector-specific, though broadly tuned recalibration of saccade gains (panel two in Fig. 4A) having a maximum average proportion of adaptation of about 0.44 (corresponding to a 11% change in saccade gain) in the direction of adaptation, dropping to 0 for saccades in the opposite direction, replicating the well-established direction-specific adaptation consistently found in this paradigm (e.g., Deubel, 1987; Frens & van Opstal, 1994). Two-way adaptation yielded a similar pattern of adaptation transfer, but affecting both leftward- and rightward saccades (panel three in Fig. 4A). Thus, adaptation was strongest near the adapted, horizontal saccade directions and somewhat weaker for vertical saccades. In all conditions, the directional extent of the adaptation is broader in the downward direction. The individual data contributing to these averages (shown in Fig. 4B) and similar individual data in other studies (Deubel, 1987; Frens & van Opstal, 1994) suggest that this biased pattern is not an exception.

The top row of panels in Fig. 4C shows the mean differences in the proportion of adaptation as a function of target direction and for all combinations of conditions: Global vs. One-way, Two-way vs. One-way, and Global vs. Two-way adaptation. The scale ranges between −0.5 and 0.5 (corresponding to ±12.5% change in saccade gain), with positive values depicting greater adaptation in the first than in the second condition. Departures of the shaded 95% confidence band from zero (the center ring highlighted in dark gray in each polar plot) reveal significant differences between conditions. As shown in the first polar plot of Fig. 4C, Global adaptation affected saccade gains much stronger than One-way adaptation for all saccade directions except a wedge of about 60° sourrounding the saccade direction adapted in One-way adaptation. Also, adaptation is greater in the Two-way than in the One-way condition (second polar plot in Fig. 4C), but only for saccades opposite the direction of the adapted saccade vector in the One-way condition. Finally, Global adaptation achieves significantly greater adaptation in the vertical directions as compared to Two-way adaptation (third polar plot in Fig. 4C). Global adaptation was not inferior to Two-way adaptation in any direction.

We conducted equivalent analyses on the transfer of adaptation across different saccade amplitudes. The results are shown in the bottom panels of Fig. 4A. Across saccade amplitudes, as across saccade directions Global adaptation resulted in stronger adaptation than the two other conditions (bottom panels in Fig. 4C). The level of adaptation was largely independent of the amplitude of the saccade target step. This could be expected for the Global adaptation condition, but we found the same amplitude-independence for the One-way and Two-way conditions and even for test saccades within ±30° of the direction that was adapted in the One-way condition (dashed lines), in line with a general gain control mechanism affecting saccades of all amplitudes (Deubel, Wolf, & Hauske, 1986; Deubel, 1987).[2]

[2] An analysis of all subjects' data combined suggested that adaptation showed some selectivity as a function of saccade amplitude in the adapted directions but the test of these 2D-landscapes versus the equivalent landscape with gain equalized along each direction (set to the mean at that direction so having no amplitude-specific pattern) showed no significant difference. So we conclude that the amplitude specific pattern did not reach significance.

3.4. Global adaptation is not accumulated vector-based adaptation

We observed a global change in saccade gains in the Global adaptation condition, which may be the result of either (1) a recalibration of saccade gains accumulating across many individually adapted vectors or (2) a fast and global recalibration mechanism. The fact that the direction-independent recalibration of saccade gains in the Global adaptation condition was of a similar magnitude and developed at a comparable speed as the direction-specific adaptation in the One-way condition render the first hypothesis unlikely; further analyses let us reject it. First, we show that the amount of adaptation accumulated in the Global condition is significantly higher than that in the other conditions. Second, based on our results in the One-way condition, we simulate an accumulation of adaptation across many directions and show that this simulation falls short of predicting the results of our Global adaptation condition.

3.4.1. Amount of accumulated adaptation

One direct test of the accumulation hypothesis is to compute and compare the area under the curve for all three conditions. Indeed, the far greater adaptation resulting from global adaptation is evidenced by the fact that when taking the area under the curve as a proxy, Global condition accumulated 2.44 ± 0.91 (mean and 95% confidence intervals) times as much adaptation as the One-way condition, and even 1.35 ± 0.18 times that in the Two-way condition. Since confidence intervals of these ratios do not overlap with 1, these differences are significant. Two-way adaptation was 1.81 ± 0.66 times as strong as One-way adaptation, again different from 1. The expected sum of two individual One-way adaptation processes is 2, well within the confidence limits of this ratio.

In the analysis of adaptation as a function of saccade amplitude, the Global condition accumulated 2.39 ± 0.89 times as much adaptation as the One-way condition, and 1.32 ± 0.16 times that in the Two-way condition. Again, since confidence intervals of these ratios do not overlap with 1, these differences are significant. Two-way adaptation was 1.93 ± 0.63 times as strong as One-way adaptation. This ratio is significantly different from 1. It is, however, very close to 2, the expected sum of two individual One-way adaptation processes, showing that unlike the Global adaptation condition, the Two-way adaptation, can be explained as an accumulation of direction-selective adaptation that is estimated from the One-way data.

3.4.2. Simulation of global adaptation as accumulation of vector-specific adaptation

The result that Global adaptation accumulated more than two times the adaptation achieved in the One-way condition while evolving at a similar (or faster) speed suggests that one can not explain the adaptation in the Global condition from the characteristics of One-way adaptation. To test this idea directly, we ran simulations of a simple, data-driven dynamic model generating predictions for the speed and magnitude of Global adaptation if it had been a result of accumulated direction-specific adaptation. First, we quantified the spatial properties of adaptation in the One-way condition. To do this, we took all subjects' data and fit a von Mises shaped function to the strength of the adaptation as a function of target direction. The von Mises distribution is the circular version of a normal distribution and is given by

$$M(\phi|\mu,\kappa) = \frac{e^{\kappa\cos(\phi-\mu)}}{2\pi I_0(\kappa)}, \tag{2}$$

where κ defines the width of the circular distribution (for $\kappa = 0$ values are uniformly distributed across angles ϕ), μ is the direction of the maximum of the distribution, and I_0 is a modified Bessel function of order 0. While μ and κ define the shape of the data, we introduce two additional parameters, γ_M and β, which allow to scale and offset the obtained von Mises distribution, respectively.

The resulting function, fitted to the One-way data, can be written as follows:

$$M_{One}(\phi|\mu,\kappa,\beta,\gamma_M) = \beta + \gamma_M e^{\kappa\cos(\phi-\mu)}, \tag{3}$$

which we will henceforth refer to as $M_{One}(\phi)$. We can incorporate the spatial and temporal characteristics of One-way adaptation into a model in order to simulate the system's behavior when given the global saccadic adaptation paradigm as input. Because saccadic adaptation is driven by post-saccadic visual error (Noto & Robinson, 2001; Wallman & Fuchs, 1998) on a trial-by-trial basis (Srimal et al., 2008), any model of saccadic adaptation should incorporate this visual error signal and the current state of adaptation. For One-way adaptation, we know both the time course of adaptation and its resultant directional profile and these are used as the parameters of a simple leaky-integrator model,

$$A(\phi,t+1) = \left(1-\frac{1}{\tau_{One}}\right)A(\phi,t) + \frac{1}{\tau_{One}}M_{One}(\phi-\phi_t), \tag{4}$$

where the adaptation for any direction ϕ at trial $t+1$, $A(\phi, t+1)$, is computed as the weighted average of the current state of adaptation for that direction, $A(\phi, t)$, and the incurred input signal (visual error) impinging on that direction, $M_{One}(\phi - \phi_t)$, i.e., $M_{One}(\phi)$ shifted by the current target direction ϕ_t. In this model, the input signal has a strong impact at early trials, driving adaptation at a high speed, but as adaptation accumulates the input's influence diminishes, leading to a saturation of the adaptation process. Both $M_{One}(\phi)$ and τ_{One} were derived from the results of the One-way condition and so this model, when run with an input sequence corresponding to a One-way condition experiment, reproduces the time-course and directional extent of One-way adaptation (see Fig. 5A and C; note that in this illustration, for the sake of comparability, we express the proportion of adaptation relative to the asymptotic adaptation obtained for rightward saccades in the One-way condition).

If the results of our Global condition are explicable from the results of the One-way condition, using a sequence of adapting saccades from a Global condition experiment this model should produce the results from our Global condition. However, if Global saccadic adaptation engages additional adaptive processes, One-way adaptation cannot explain the full extent of the results of our Global condition. In this case, this simulation should result in less adaptation than is the case in the One-way condition. Note that here we have assumed that adaptation is not amplitude-specific, an assumption that is known to be incorrect (Watanabe et al., 2000). However, we find no evidence of this amplitude specificity in our data, so for reasons of simplicity we chose to omit this factor.

Fig. 5B and C show that running the simulation described above, using an input pattern taken from an actual Global adaptation experiment, i.e., a random sequence of target directions (see lower panel in Fig. 5C), results in far lower levels of adaptation (solid red lines) than is actually the case in the Global condition (dashed red lines). Clearly, Global adaptation when built up out of accumulated vector-specific adaptation as found in the One-way condition does not explain the amount of adaptation we found in our Global condition experiments. This result indicates that Global saccadic adaptation involves additional adaptive processes.

4. Discussion

We introduced a generalized version of the classical saccadic adaptation paradigm, providing a consistent postsaccadic cue to miscalibration of saccade gain in all directions. In response to this

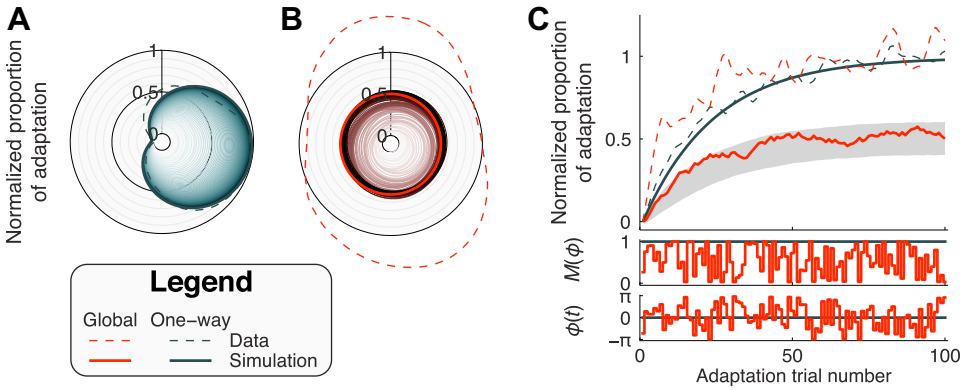

Fig. 5. Results obtained from a simulation of the leaky-integrator model. **A** and **B** Final spatial extent (thick lines) of One-way (**A**) and Global (**B**) adaptation for the simulation run shown in panel **C**. Thin solid lines depict the gradual change in adaptation as across trials; brighter colors depict earlier trials. Dashed lines provide the actual average data for reference (as reported in Fig. 4A). **C** Time course of adaptation for rightward saccades (the results for Global adaptation hold for all saccade directions). During adaptation, One-way and Global condition sequences of input (middle panel) differ. The stimulation protocol in the One-way condition provides constant high input for the adaptation of rightward saccades (black), whereas the global condition's stimulation protocol provides weaker and highly variable input (red), due to varying target angles, $\phi(t)$, in the Global condition (lower panel). The simulated time-course of adaptation (upper panel) in the Global condition (red solid line; shaded area provides 95% confidence interval across 1000 simulation runs), compared to the adaptation in this direction in the One-way condition (black solid lines) mirrors the difference between the input patterns. Again, dashed lines provide the actual average data for reference (as reported in Fig. 3B). Clearly, accumulated vector-based adaptation does not account for the high levels of adaptation found in the Global condition (dashed red line). Note that for the sake of comparability, the proportion of adaptation was normalized, i.e., expressed relative to the asymptotic adaptation obtained for rightward saccades in the One-way condition. (For interpretation of the references to color in this figure legend, the reader is referred to the web version of this article.)

cue, we observe a fast and powerful recalibration process for saccadic eye movements, globally reducing the gain for all saccade vectors tested. We also replicated the well-documented finding of direction-specific adaptation in our One-way condition (Albano, 1996; Alahyane et al., 2008; Collins et al., 2007; Deubel, 1987; Frens & van Opstal, 1994; Noto et al., 1999; Miller et al., 1981; Straube et al., 1997). Clearly, this vector-based adaptation can not account for our results, because adaptation in the One-way condition would have had to be significantly stronger than adaptation in the Global condition. That was not the case. Despite the fact that a broad range of saccade vectors was adapted in the Global adaptation condition, adaptation proportion developed at a similar speed as in the One-way adaptation condition, and similar asymptotes for the adapted saccades were achieved in both conditions. If anything, our time course analyses indicate a slightly faster recalibration of saccade gains in the Global adaptation condition, suggesting that the underlying processes, even though affecting all vectors in general and accumulating almost 2.5 times as much adaptation, are not slower than those implementing vector-specific adaptation. This conclusion is corroborated by the fact that the attempt to model Global adaptation as accumulating vector-based adaptation resulted in less than half the adaptation observed in that condition. So, without specifically adapting saccades of a certain direction and amplitude (but adapting many others), these saccades are adapted equally strongly using Global adaptation as when they were explicitly adapted using the traditional paradigm.

Two potential mechanisms for global adaptation are possible (1) the presence of consistent error signals rather than the inconsistent error signals in the traditional one-way adaptation where one direction is adapted but the return is not; and (2) the existence of a general gain control for all saccades. The results of the Two-way adaptation condition studied here enable us to evaluate the relative contributions of these two factors. In this condition, consistent feedback was provided for all saccades triggered during adaptation, yet these saccades were always in two opposite directions. The first of the above hypotheses would predict a similar transfer of adaptation as in the Global adaptation condition. However, transfer in the Two-way adaptation condition closely mimicked the combination of two One-way adaptation processes, replicating earlier findings (Deubel, 1987). Moreover, large differences in adaptation were obtained between Global and Two-way adaptation for saccade directions furthest from those adapted in Two-way adaptation. We conclude, therefore, that vector-specificity is or has evolved to be (by accumulation of evidence across trials that specific saccade directions need a gain change) the dominant factor in Two-way adaptation. Alternatively, vector-specificity in the Two-way condition may be the result of inconsistent error feedback for non-adapted directions, which are only triggered in non-adapting test trials. Thus, adaptation in these directions may have quickly recovered during the first test trials. A re-analysis of our data rendered this possibility unlikely: Even if only the first few post-adaptation test trials were analyzed, we obtained similar directional transfer (see Fig. 6).

A fast global recalibration mechanism of saccade gains seems at odds with results from a study by Scudder et al. (1998). These authors compared saccadic adaptation when monkeys made saccades to random locations in either a 1 by 2 or a 5 by 3 position grid of possible target locations. In that study, adaptation was found to evolve slower if more target locations were possible, as predicted by an accumulation of multiple vector-based adaptation processes. Unfortunately, the authors collapsed hundreds of adaptation trials into a single data point, veiling any potential fast adaptation mechanisms if they were present. Moreover, the differences between their study and ours are numerous, including

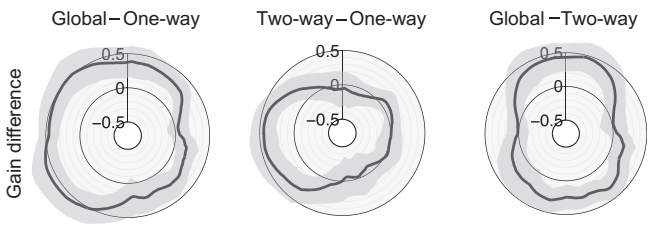

Fig. 6. Differences in the proportion of adaptation between Global – One-way adaptation, Two-way – One-way adaptation, and Global – Two-way adaptation are shown as a function of target step direction when analyzing only the first 20 test trials of the post-adaptation block. Conventions as in Fig. 4C. Despite a higher level of noise resulting from the reduced amount of data, the differences between conditions closely mimic those obtained using the entire set of test trials.

species and procedure. One difference that we feel could be critical is that we found the global adaptation when the direction and amplitude of target steps were unpredictable whereas the target steps in Scudder et al's procedure were highly predictable (there were strong biases in amplitude and direction). This predictability may have favored the contribution of the direction-specific saccade adaptation mechanisms over any global mechanism.

What is a likely neural locus of global saccadic gain adaptation? Many previous studies of saccadic adaptation have focused on oculomotor areas that encode saccades as a vector rather than their components (review in Hopp & Fuchs, 2004), pre-eminently the SC, the most peripheral of these structures. Recent evidence suggests that amplitude changes in saccade adaptation are accompanied by changes in firing rates and/or movement fields of corresponding SC neurons (Takeichi, Kaneko, & Fuchs, 2007). These changes may either be a manifestation of amplitude recalibration, or themselves trigger oculomotor learning further downstream (Kaku et al., 2009). Due to its vector specificity, the SC is no likely candidate for a general recalibration mechanism, unless consistent visual cues to miscalibration for all saccades result in a super-additive lateral potentiation of learning, affecting many (or all) SC neurons concurrently. More likely, Global adaptation triggered learning in more peripheral sites, including the cerebellar fastigial oculomotor region, which strongly projects to saccadic burst neurons in the brainstem (Scudder, McGee, & Balaban, 2000). At this final stage of oculomotor processing, the duration of bursts projected to motorneurons controlling the extraocular muscles linearly relates to saccade amplitude. Hence, only one parameter needs adjustment to similarly affect saccadic gain of many saccades at the same time. The properties demonstrated here for a general recalibration mechanism for saccades pinpoints these potential neurophysiological correlates and may help explain the conflicting results in many of the studies using variants of the traditional paradigm.

While it had been shown previously that motor adaptation develops simultaneously at many different temporal scales (Körding et al., 2007), our data provide evidence for the idea that goal-directed behavior unfolds and develops on many different spatial scales as well. These processes are the basis of our successful interaction with the environment, and generalization across many different motor acts, shown here for saccades in all directions, is an integral part of this plasticity.

Acknowledgments

We thank Claudia Buß for help with data acquisition. This work was supported by the 7th Framework Program of the European Commission (Marie Curie International Outgoing Fellowship 235625 awarded to M.R.) and by a Chaire d'Excellence grant to P.C.

Appendix A

A.1. Baseline correction of saccade gains

Individuals may differ in the amount of undershoot or overshoot they produce when making saccades to visual targets, and these biases in saccade gain may differ as a function of saccade direction. To determine baseline biases in saccade gain as a function of target direction we applied LOWESS regressions to the pre-adaptation test data. The proportion of adaptation of any saccade in a given target direction was then expressed relative to this baseline. Fig. 7A helps illustrating this procedure. To facilitate comparison to post-adaptation data, we will plot all data as a proportion of adaptation, that is, we will express the difference of saccade gain from 1 relative to the gain change to be induced by the intra-saccadic back-step (0.25). The gray dots in the polar plot in Fig. 7A show one observer's data from the pre-adaptation test

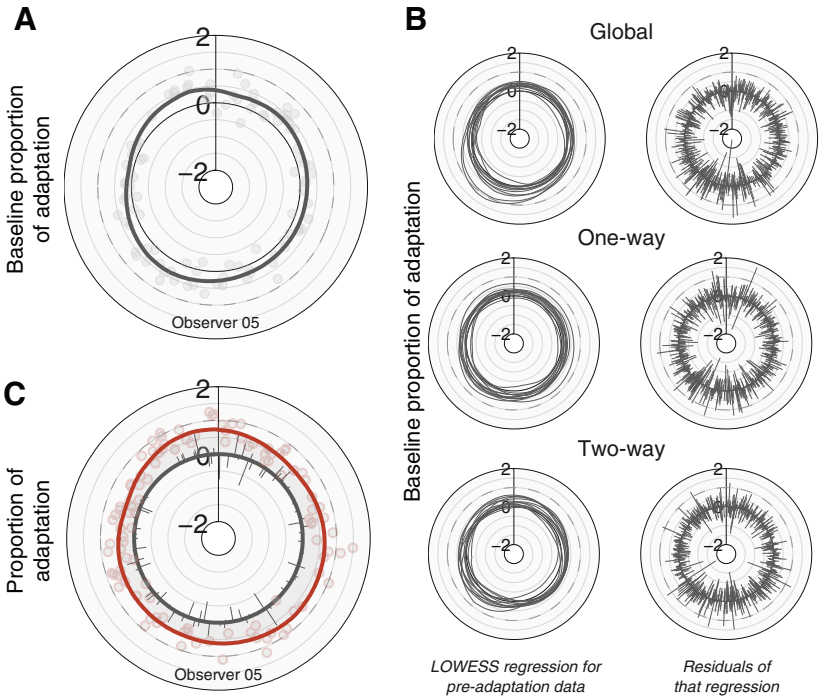

Fig. 7. Pre-adaptation data and baseline-correction. **A** Polar plot showing the baseline proportion of adaptation as a function of target direction in the pre-adaptation test block of the Global adaptation condition for one observer. Gray dots show single saccade data, the thick gray line shows the LOWESS regression. Positive values reveal that on average the observer undershot and fell slightly short of the targets. **B** Smoothed pre-adaptation baseline data from 12 observers in three conditions (left panel) and the residuals of these regressions on the data (right column) for the three conditions tested. Residuals do not reveal any systematic biases in the regression procedure. **C** Data from test trials in the post-adaptation block were expressed relative to the regression of the pre-adaptation test data (thick gray line shown with residuals; see text for details). Pink dots are single saccades; the thick red line shows the smoothed average. As highlighted by the gray shaded area, saccades in all directions had were affected by Global adaptation. (For interpretation of the references to color in this figure legend, the reader is referred to the web version of this article.)

trials in the Global adaptation condition; the thick line shows the result of the LOWESS regression. The deviation of this regression line from zero towards positive values indicates that this observer had substantial undershoot even before adaptation took place. In addition, this undershoot differs slightly as a function of saccade direction. This pattern of baseline data is a well known characteristic of rapid eye movements and was observed for many of our observers. Fig. 7B shows LOWESS regressions of the pre-adaptation test data for all observers (left column) along with the residuals (right column) for each condition separately. Plotting the baseline data as a proportion of adaptation highlights that without correcting for these individual and direction-specific biases, we might have overestimated the effects of adaptation.

Saccade amplitudes of test trials in the pre-adaptation block represent a baseline for the effects of adaptation in the adaptation and post-adaptation blocks. However, contrary to previous work on saccadic adaptation using only a limited number of target directions, we triggered saccades with random directions. Saccade gains and, thus, the proportion of adaptation differ greatly as a function of saccade direction and these dependencies vary considerably across observers and sessions (see Fig. 7B). Therefore, our measure of adaptation had to be expressed relative to the directionally specific baseline under- or overshoot obtained in the LOWESS regression of the baseline pre-adaptation data. Thus, for each observer, we computed the proportion of adaptation of each saccade relative to those in pre-adaptation test trials. The pink dots in the polar plot in Fig. 7C show the result for the same observer as in Fig. 7A, for the post-adaptation test trials following Global adaptation. The thick red line is the LOWESS regression on this data. The pre-adaptation regression is again represented by a thick gray line (now a circle, due to the baseline-correction procedure), its residuals are shown as thin gray lines protruding from it. The change in the proportion of adaptation due to Global adaptation is highlighted by the shaded area.

References

Abel, L., Schmidt, D., Dell'osso, L., & Daroff, R. (1978). Saccadic system plasticity in human. *Annals of Neurology, 4*, 313–318.

Alahyane, N., Devauchelle, A. D., Salemme, R., & Pélisson, D. (2008). Spatial transfer of adaptation of scanning voluntary saccades in humans. *Neuroreport, 19*, 37–41.

Albano, J. E. (1996). Adaptive changes in saccade amplitude: Oculocentric or orbitocentric mapping? *Vision Research, 36*, 2087–2098.

Barton, J. J., Jama, A., & Sharpe, J. A. (1995). Saccadic duration and intrasaccadic fatigue in myasthenic and nonmyasthenic ocular palsies. *Neurology, 45*, 2065–2072.

Brainard, D. H. (1997). The psychophysics toolbox. *Spatial Vision, 10*, 433–436.

Bridgeman, B., Hendry, D., & Stark, L. (1975). Failure to detect displacement of visual world during saccadic eye movements. *Vision Research, 15*, 719–722.

Cleveland, W. S. (1979). Robust locally weighted regression and smoothing scatterplots. *Journal of the American Statistical Association, 74*, 829–836.

Collins, T., Doré-Mazars, K., & Lappe, M. (2007). Motor space structures perceptual space: Evidence from human saccadic adaptation. *Brain Research, 1172*, 32–39.

Cornelissen, F. W., Peters, E. M., & Palmer, J. (2002). The eyelink toolbox: Eye tracking with MATLAB and the psychophysics toolbox. *Behavior Research Methods, Instruments, & Computers, 34*, 613–617.

Deubel, H. 1987. Adaptivity of gain and direction in oblique saccades. In: J.K. OŘegan, & A. Lévy-Schoen (Eds.), Eye movements: From physiology to cognition (pp. 181–190).

Deubel, H., Wolf, W., & Hauske, G. (1986). Adaptive gain control of saccadic eye movements. *Human Neurobiology, 5*, 245–253.

Efron, B., & Tibshirani, R. J. (1993). *An Introduction to the Bootstrap*. New York: Chapman & Hall.

Engbert, R., & Mergenthaler, K. (2006). Microsaccades are triggered by low retinal image slip. *Proceedings of the National Academy of Sciences, USA, 103*, 7192–7197.

Frens, M. A., & van Opstal, A. J. (1994). Transfer of short-term adaptation in human saccadic eye movements. *Experimental Brain Research, 100*, 293–306.

Garaas, T. W., Nieuwenhuis, T., & Pomplun, M. (2008). A gaze-contingent paradigm for studying continuous saccadic adaptation. *Journal of Neuroscience Methods, 168*, 334–340.

Hopp, J. J., & Fuchs, A. F. (2004). The characteristics and neuronal substrate of saccadic eye movement plasticity. *Progress in Neurobiology, 72*, 27–53.

Hopp, J. J., & Fuchs, A. F. (2006). Amplitude adaptation occurs where a saccade is represented as a vector and not as its components. *Vision Research, 46*, 3121–3128.

Kaku, Y., Yoshida, K., & Iwamoto, Y. (2009). Learning signals from the superior colliculus for adaptation of saccadic eye movements in the monkey. *Journal of Neuroscience, 29*, 5266–5275.

Kommerell, G., Oliver, D., & Theopold, H. (1976). Adaptive programming of phasic and tonic components in saccadic eye movements. *Investigative Ophthalmology and Visual Science, 155*, 657–660.

Körding, K. P., Tenenbaum, J. B., & Shadmehr, R. (2007). The dynamics of memory as a consequence of optimal adaptation to a changing body. *Nature Neuroscience, 10*, 779–786.

McLaughlin, S. (1967). Parametric adjustment in saccadic eye movements. *Perception & Psychophysics, 2*, 359–362.

Miller, J., Anstis, T., & Templeton, W. (1981). Saccadic plasticity: Parametric adaptive control by retinal feedback. *Journal of Experimental Psychology, 7*, 356–366.

Noto, C. T., & Robinson, F. R. (2001). Visual error is the stimulus for saccade gain adaptation. *Cognitive Brain Research, 12*, 301–305.

Noto, C. T., Watanabe, S., & Fuchs, A. F. (1999). Characteristics of adaptation fields produced by behavioral changes in saccadic gain and direction. *Journal of Neurophysiology, 81*, 2798–2813.

Optican, L., & Robinson, D. (1980). Cerebellar-dependent adaptive control of primate saccadic system. *Journal of Neurophysiology, 44*, 1058–1079.

Pelli, D. G. (1997). The VideoToolbox software for visual psychophysics: Transforming numbers into movies. *Spatial Vision, 10*, 437–442.

Scudder, C. A., Batourina, E. Y., & Tunder, G. S. (1998). Comparison of two methods of producing adaptation of saccade size and implications for the site of plasticity. *Journal of Neurophysiology, 79*, 704–715.

Scudder, C. A., McGee, D. M., & Balaban, C. D. (2000). Connections of monkey saccade-related fastigial nucleus neurons revealed by anatomical and physiological methods. *Society for Neuroscience Abstracts, 26*, 971.

Snow, R., Hore, J., & Vilis, T. (1985). Adaptation of saccadic and vestibulo-ocular systems after extraocular muscle tenectomy. *Investigative Ophthalmology and Visual Science, 26*, 924–931.

Sparks, D. L. (2002). The brainstem control of saccadic eye movements. *Nature Reviews Neuroscience, 3*, 952–964.

Srimal, R., Diedrichsen, J., Ryklin, E. B., & Curtis, C. E. (2008). Obligatory adaptation of saccade gains. *Journal of Neurophysiology, 99*, 1554–1558.

Straube, A., Fuchs, A. F., Usher, S., & Robinson, F. R. (1997). Characteristics of saccadic gain adaptation in rhesus macaques. *Journal of Neurophysiology, 77*, 874–895.

Takeichi, N., Kaneko, C. R., & Fuchs, A. F. (2007). Activity changes in monkey superior colliculus during saccade adaptation. *Journal of Neurophysiology, 97*, 4096–4107.

Wallman, J., & Fuchs, A. F. (1998). Saccadic gain modification: Visual error drives motor adaptation. *Journal of Neurophysiology, 80*, 2405–2416.

Warabi, T., Kase, M., & Kato, T. (1984). Effects of aging on the accuracy of visually guided saccadic eye movements. *Annals of Neurology, 16*, 449–454.

Watanabe, S., Noto, C. T., & Fuchs, A. F. (2000). Flexibility of saccade adaptation in the monkey: Different gain states for saccades in the same direction. *Experimental Brain Research, 130*, 169–176.